DOI: 10.1093/brain/awg196 Advanced Access publication June 23, 2003 *Brain* (2003), **126,** 1955–1967

Dissociating atrophy and hypometabolism impact on episodic memory in mild cognitive impairment

Gaël Chételat,[1] Béatrice Desgranges,[1] Vincent de la Sayette,[1,2] Fausto Viader,[1,2] Karim Berkouk,[1,3] Brigitte Landeau,[1] Catherine Lalevée,[1,2] François Le Doze,[2] Benoît Dupuy,[4] Didier Hannequin,[5] Jean-Claude Baron[2,7] and Francis Eustache[1,6]

[1]*INSERM E0218-Université de Caen, GIP Cyceron, CHU Côte de Nacre,* [2]*Services de Neurologie, CHU de Caen,* [3]*PVE-OUT EC project,* [4]*CH de Cherbourg,* [5]*CHU de Rouen,* [6]*Ecole Pratique des Hautes Etudes, CNRS 8581, Université René Descartes, Paris 5, France and* [7]*Department of Neurology, University of Cambridge, Cambridge, UK*

Correspondence to: Professor Francis Eustache, INSERM E0218-Université de Caen, Laboratoire de Neuropsychologie, CHU Côte de Nacre, 14033 Caen cedex, France
E-mail: neuropsycho@chu-caen.fr

Summary

The present study aims to unravel, in the same study, both morphological and functional specific substrates of encoding versus retrieval deficits in patients with amnestic mild cognitive impairment (MCI). For this purpose, 21 highly screened MCI patients with isolated memory impairment, who attended a memory clinic and fulfilled operational criteria for MCI, underwent (i) two episodic memory subtests designed to assess preferentially either incidental encoding or retrieval capacity; (ii) a high-resolution T_1-weighted volume MRI scan; and (iii) a resting state [^{18}F]fluoro-2-deoxy-D-glucose PET study. Using statistical parametic mapping, positive correlations between memory scores on one hand, and grey matter density and normalized partial volume effect-corrected brain glucose utilization (ncCMRglc) on the other hand, were computed. Deficits in both encoding and retrieval were correlated with declines in hippocampal region grey matter density. The encoding subtest also correlated with hippocampal ncCMRglc, whereas the retrieval subtest correlated with the posterior cingulate area ncCMRglc only. The present findings highlight a distinction in the neural substrates of encoding and retrieval deficits in MCI. Furthermore, they unravel a partial dissociation between metabolic and structural correlates, suggesting distinct interpretations. Hippocampal atrophy was related to both encoding and retrieval deficits, possibly reflecting a direct effect on hippocampal functioning, as well as an indirect effect, through remote functional disruption, on posterior cingulate region synaptic function, respectively.

Keywords: Alzheimer's disease; resting cerebral glucose metabolism; MRI; statistical parametric mapping; episodic memory

Abbreviations: ^{18}FDG = [^{18}F]fluoro-2-deoxy-D-glucose; GM = grey matter; HCP = hippocampal area; MCI = mild cognitive impairment; MMSE = Mini-Mental State Examination; ncCMRglc = normalized and partial volume effect-corrected cerebral glucose utilization; PVE = partial volume effect; SPM = statistical parametric mapping; VBM = voxel-based morphometry; WM = white matter

Introduction

While Alzheimer's disease affects a considerable and increasing part of the population, the potential for disease-controlling treatment has led to recent efforts to identify Alzheimer's disease as early as possible. Hence, the pre-dementia stage of the disease has become a major topic of current research. Amnestic 'mild cognitive impairment' (MCI) has recently emerged as the most convenient avenue to address this issue, since most MCI patients will progress to Alzheimer's disease, at a rate of 10–15% per year, suggesting that it represents the clinical manifestation of incipient Alzheimer's disease (Petersen *et al*., 2001).

Amnestic MCI is characterized by a selective impairment of episodic memory function beyond that expected for age. Episodic memory deficit is a feature of normal ageing too, mainly involving retrieval strategy, and is also the earliest and most severe cognitive deficit in Alzheimer's disease, but here

principally involving encoding (Carlesimo *et al*., 1998; Deweer *et al*., 2001). Interestingly, it remains unclear which aspect of episodic memory is most vulnerable in MCI. The similar intensity of recognition and free recall impairments suggests that encoding deficits may predominate, whereas retrieval problems may not be the major source of episodic memory impairment at this stage (Almkvist *et al*., 1998). This idea is reinforced further by the recent study of Wang and Zhou (2002). Assessing MCI patient performances as compared with age-matched controls in two tasks designed to assess preferentially encoding versus retrieval capacity, these authors showed the impairment to be major in the former (23%; $P < 0.001$), but milder in the latter (7%; $P = 0.02$). They used an experimental procedure based on a previous functional imaging study on normal subjects, showing that encoding versus retrieval processes involved distinct neural systems (Gabrieli *et al*., 1997). Altogether, these results suggest that episodic memory deficits in MCI and Alzheimer's disease versus ageing may be related to preferential encoding versus retrieval deficit, respectively, and thus may be related to different substrates of neural alteration.

This hypothesis is reinforced by neuroimaging studies. Structural MRI measures, as well as PET data of resting brain glucose utilization, can be correlated with cognitive performances so as to unravel the structural and functional substrates of memory impairment. First, while most studies in normal ageing failed to evidence statistically significant correlation between medial temporal lobe volume and episodic memory impairment (see for example Raz *et al*., 1998; Petersen *et al*., 2000), this relationship has been documented consistently in early Alzheimer's disease (for a review see Deweer *et al*., 2001). Secondly, metabolic PET correlative studies pointed to an involvement of the prefrontal cortex in normal ageing (Eustache *et al*., 1995; Langley and Madden, 2000; Deweer *et al*., 2001) and of the medial temporal lobe, but also of other structures such as the thalamus and posterior cingulate gyrus, in early Alzheimer's disease (Perani *et al*., 1993; Desgranges *et al*., 1998*a*, 2002; Eustache *et al*., 2001). The central role of the posterior cingulate cortex in episodic memory (Cabeza and Nyberg, 2000), together with its specific metabolic alteration in amnestic MCI patients and early Alzheimer's disease patients (for a review see Matsuda, 2001), also suggest the implication of this structure in episodic memory deficits in Alzheimer's disease. Altogether, these studies further argue in favour of a distinction in the cerebral alteration processes subtending episodic memory deficits in normal ageing versus Alzheimer's disease.

Thus, assessing the brain structures specifically involved in the memory deficits of MCI patients would be of interest to elucidate further the pathological processes underlying cognitive dysfunction at this pre-dementia stage. To date, however, only one study has assessed the correlations between MRI volumetric measurements of temporal lobe structures and memory performance in MCI (Convit *et al*., 1997). The authors reported significant positive correlations between hippocampal atrophy and verbal delayed recall deficit. In a book chapter, the same group reported similar findings with medial temporal lobe glucose metabolism (De Santi *et al*., 1995). These studies suggest the involvement of the hippocampal area (HCP) in episodic memory impairment of MCI patients. However, they did not focus on amnestic MCI. Furthermore, differentially assessing encoding versus retrieval processes was not the topic of these studies. Above all, both studies used the regions-of-interest approach, focusing on the temporal lobe and leaving unexplored large areas of the brain.

In this respect, voxel-by-voxel analysis, such as with statistical parametric mapping (SPM), is a promising alternative to provide a prospective and fully comprehensive assessment of the brain without bias. First, it allows assessment of the entire brain, thus reinforcing the specificity of the findings. Secondly, it gives an account of the precise localization of the area concerned, as only significant pixels would be detected. Furthermore, this stereotactic localization approach is applicable both to functional and, with the more recently emerged voxel-based morphometry (VBM; see Ashburner and Friston, 2000; Good *et al*., 2001), to structural cerebral data sets, thus providing a unique way to assess both issues concomitantly. VBM has been validated by using independent methodology (Wright *et al*., 1999), and already used to examine brain structural changes notably in Alzheimer's disease (Baron *et al*., 2001*a*). The correlative approach between cognitive scores and brain metabolism in Alzheimer's disease using SPM has also shown results consistent with those obtained using the classic regions-of-interest approach (Desgranges *et al*., 1998*a*).

Our aim in this study of amnestic MCI was to assess, using SPM, the relationships between brain alterations, as measured by both structural MRI and functional PET, and episodic memory performances, as assessed by an original neuropsychological paradigm designed to probe preferentially either encoding or retrieval. Our main objectives were: (i) to identify the specific neural substrates underlying encoding versus retrieval deficits in MCI; and (ii) to dissociate atrophy versus hypometabolism impact on these memory processes.

Patients and methods

Recruitment and selection of patients

Twenty-one patients with amnestic MCI (Petersen *et al*., 2001) were examined in this study. All were exclusively right-handed according to the Edinburgh inventory (Oldfield, 1971), except one patient who scored 67%. They were all recruited prospectively through a memory clinic, and all complained of memory impairment. They underwent medical, neurological, neuropsychological and neuroradiological examinations, and were selected according to the following stringent criteria: (i) lack of present or historical evidence of significant neurological, psychiatric or medical disease, use of medication that could affect brain functioning or structure,

Table 1 *Characteristics of the MCI patients and healthy control (HC) samples used for memory score (HC1), grey matter density (HC2) and ncCMRglc data (HC3) comparisons*

	MCI	HC1	HC2	HC3
Number	21	30	22	13
Age (years): mean ± SD	71.2 ± 8.1	68.2 ± 3.9	66.6 ± 7.2	63 ± 9.7*
(range)	(55–87)	(64–83)	(59–83)	(51–83)
Percentage female	57	60	55	54
Education (years): mean ± SD	9.8 ± 3.5	9.7 ± 2.4	10.2 ± 3.8	10.8 ± 2.6
(range)	(7–17)	(6–15)	(7–17)	(7–15)
MMSE: mean ± SD	27.3 ± 1.4	–	–	–
(range)	(24–29)			

MMSE: Mini-Mental State Examination. Significant differences ($P < 0.05$; two-sample t test) relative to MCI are indicated by asterisks.

and depression or substance abuse; (ii) modified Hachinski ischaemic score ⩽2 (Loeb and Gandolfo, 1983); (iii) age over 55 years; (iv) objective memory impairment, as defined by performance 1.5 SD below the normal mean for age-matched controls in at least one subscore of the Grober and Buschke test (Grober and Buschke, 1987) or in the Rey's figure delayed recall test (Rey, 1959); and (v) NINCDS-ADRDA criteria for probable Alzheimer's disease (McKhann *et al*., 1984) not met, as assessed by an extensive neuropsychological examination including measurements of general intellectual function, i.e. Mini-Mental State Examination (MMSE; Folstein *et al*., 1975), and of cognitive functions other than episodic memory, including executive (Stroop test; Golden, 1978), visuospatial (copy of Rey's figure; Rey, 1959) gestural praxis (imitation of four meaningless gestures, production of four symbolic gestures and four object utilization gestures), language (writing of 12 irregular words under dictation) and image naming (DO80; Deloche and Hannequin, 1997) functions. Each patient gave written informed consent to participate in the study, which was approved by the regional ethics committee (CCPP RB-Corsité Consultatif de Protection des Personnes dans la Recherche Biomédicale de Base-Normandie). The characteristics of the MCI group are listed in Table 1.

Within a few days interval at most, each of the 21 MCI patients underwent (i) an episodic memory test especially designed for the correlative analysis; (ii) a PET study using [^{18}F]fluoro-2-deoxy-D-glucose (^{18}FDG); and (iii) a high-resolution T_1-weighted volume MRI scan.

Episodic memory assessment

To tax preferentially encoding or retrieval episodic memory processes, we used the 'Encoding, Storage, Retrieval' paradigm of Eustache *et al*. (1998), which includes two learning phases (one superficial and one deep) of two different word lists. Each list comprised 16 words, belonging to 16 different semantic categories. The words were concrete nouns of 5–8 letters, with a lexical frequency ranging from 100 to 10 000, selected from the Brulex French lexical data bank (Content *et al*., 1990). For the first list, patients had to say whether the first and last letters of each orally presented word were in alphabetical order, without any instruction to memorize. At the end of this incidental superficial encoding phase, a recognition phase was carried out where patients had to recognize the 16 target words among distractors. Each target word was presented visually, one by one, with three distractors, one semantically linked, one phonetically linked, and the third with no link with the target word. For each of these 16 presentations, patients were systematically required to point to a word with their finger, the one they recognized, or otherwise the one they chose at random. For the second list, patients were asked to memorize the words. In order to induce a semantic processing, they had to generate orally a sentence that defined or described the orally presented word. Every two words, an immediate cued recall task was performed using a semantic category cue, in order to ensure that encoding was made and to reinforce its semantic nature. If the patient failed, he was reminded of the word, and again requested to make a sentence containing the target, and to recall it in response to its categorical cue. At the end of this 16-word intentional deep encoding, patients were asked to recall as many words as possible, in any order and without time limitation.

The total number of correctly recognized words of the first list and of recalled target words of the second list was calculated, resulting in the following two subscores: recognition after incidental superficial encoding, and free recall after intentional deep encoding. Each of these subscores is assumed to reflect preferentially a subject's capacity in a particular process of episodic memory. Thus, the recognition after the superficial encoding subtest, where retrieval was made easier by presentation of the target, thereby mostly compensating for potential retrieval deficits, whereas encoding was not supported, is assumed to be more dependent on encoding ability. In contrast, the free recall after the deep encoding subtest, which represents the inverse situation, with encoding being reinforced while retrieval was self-initiated, is assumed to reflect mainly retrieval ability. Although it is recognized that these subtests do not constitute pure measures of either encoding or retrieval capacity, and hence only represent one form of each process (i.e. incidental encoding

and effortful retrieval), they will be designated in what follows by the process they preferentially tax (i.e. 'encoding' and 'retrieval' subtests) for the sake of simplicity (Gabrieli *et al*., 1997).

MRI data acquisition

All MCI patients underwent a high-resolution T_1-weighted volume MRI scan, which consisted of a set of 128 adjacent axial cuts parallel to the anterior–posterior commissure (AC–PC) line and with slice thickness 1.5 mm and pixel size 1 × 1 mm, using the SPGR (spin gradient recalled) gradient echo sequence (repetition time, TR = 15.4 s; echo time, TE = 3.4 kHz; field of view, FOV = 24 cm; matrix = 256 × 256). All the MRI data sets were acquired on the same scanner (1.5 T Signa Advantage echospeed; General Electric) and with the same parameters. Standard correction for field inhomogeneities was applied.

PET data acquisition

All MCI patients underwent a PET study using ^{18}FDG. Data were collected using the high-resolution PET device ECAT Exact HR+ with isotropic resolution of 4.6 × 4.2 × 4.2 mm (FOV = 158 mm). The patients were fasted for at least 4 h before scanning. To minimize anxiety, the PET procedure was explained in detail beforehand. The head was positioned on a headrest according to the cantho-meatal line and gently restrained with straps. ^{18}FDG uptake was measured in the resting condition, with eyes closed, in a quiet and dark environment. A catheter was introduced in a vein of the arm to inject the radiotracer. Following ^{68}Ga transmission scans, 3–5 mCi of ^{18}FDG were injected as a bolus at time 0, and a 10 min PET data acquisition started at 50 min post-injection. Sixty-three planes were acquired with septa out (volume acquisition), using a voxel size of 2.2 × 2.2 × 2.43 mm (x, y, z). During PET data acquisition, head motion was continuously monitored with, and whenever necessary corrected according to, laser beams projected onto ink marks drawn over the forehead skin.

Image handling and transformations

MRI data

MRI data were analysed using the fully automated VBM procedure (Ashburner and Friston, 2000), recently optimized by Good *et al*. (2001). The several pre-processing steps, namely creation of customized whole brain and grey matter (GM) templates, spatial normalization, segmentation, brain extraction and smoothing, have been described in detail (Ashburner and Friston, 2000, 2001; Good *et al*., 2001). Briefly, before subjecting the original whole brain structural images to the three classical steps of normalization, segmentation and smoothing, three pre-processing steps were performed. In the first step, a whole brain template was created from the whole MCI sample by spatially normalizing each original structural MRI to the standard SPM-99 T_1 template, smoothing the normalized data with an 8 mm full-width at half-maximum isotropic Gaussian kernel, and creating a mean image (the template) from these 21 normalized and smoothed images. The second step was the creation of a customized GM template, which implied the normalization of each original whole brain data set to the previously created template, the segmentation of these normalized data into GM, white matter (WM), CSF and other non-brain partitions, the 12 mm full-width at half-maximum smoothing of GM data, and the averaging of the 21 smoothed normalized GM images. In the third step, optimized normalization parameters were determined according to the following stages: (i) segmentation of the original structural images (in native space) to isolate the GM set; (ii) extraction (erosion and conditional dilatation) of the GM set so as to remove unconnected non-brain voxels (scalp, skull and dural venous sinus) from the segmented images; and (iii) spatial normalization of this extracted GM partition using the customized GM template created in the second step, thus providing the optimal spatial normalization parameters. Once these pre-processing steps were completed, the whole brain structural data sets (in native space) were spatially normalized, reapplying the pre-determined optimized normalization parameters, and segmented into GM, WM, CSF and non-CSF partitions. Normalized segmented GM images were then subjected to a second extraction step, before being smoothed using a 12 mm full-width at half-maximum kernel. The resulting images will be referred to as 'GM density' data in what follows.

PET data

Correction for partial volume effect (PVE). The PET data were corrected for PVE due to both CSF and WM using the optimal voxel-by-voxel method originally proposed by Müller-Gartner (1992). Briefly, the original MRI data sets were first segmented into GM, WM and CSF using SPM-99. The whole brain MRI data, as well as the GM, WM and CSF partitions were then co-registered and resliced to the PET data (using the mutual information option in SPM-99, as recommended when images have been acquired in different modalities; Ashburner and Friston, 1997). To generate a virtual PET image of the WM, a PET value of the WM was extracted from the centre of the centrum semiovale (where PVE is thought to be minimal) and applied to the WM map degraded to the PET resolution ('smoothed' WM map) using the point spread function of the PET scanner. Voxel by voxel, the virtual PET image of the WM was then subtracted from the original PET data, and the resulting image was divided by the 'smoothed' GM map, thus providing a PET image of the GM, corrected for PVE due to WM and CSF.

Handling. Using SPM (SPM-99; Wellcome Department of Cognitive Neurology, London, UK), the PVE-corrected PET data were subjected to an affine and non-linear spatial

Table 2 *Peak Talairach coordinates of the significant (P voxel-level <0.005; P cluster-level <0.01; uncorrected) positive correlations between GM density or ncCMRglc and performances in the encoding and retrieval episodic memory subtests (principal analyses)*

$P_{corrected}$ (cluster-level)	*k*	Regions	Coordinates (mm)			$P_{uncorrected}$ (voxel-level)	*Z*
			x	*y*	*z*		
Encoding subtest: correlations with GM density							
0.132	279	R amygdala	30	–3	–18	<0.001	3.77
		R superior temporal gyrus	42	–4	–12	0.002	2.83
Encoding subtest: correlations with ncCMRglc							
0.109	329	R hippocampus	28	–28	–10	0.001	3.06
		R superior temporal gyrus	42	–20	–7	0.001	2.97
		R hippocampus	34	–13	–20	0.002	2.92
Retrieval subtest: correlations with GM density							
0.062	340	R hippocampus	34	–26	–7	<0.001	3.68
		R amygdala	28	–9	–15	<0.001	3.39
0.024	431	L hippocampus	–26	–14	–14	<0.001	3.54
		L hippocampus	–38	–28	–12	0.001	3.02
Retrieval subtest: correlations with ncCMRglc							
0.007	654	L posterior cingulate gyrus	–6	–55	29	<0.001	3.75
		R posterior cingulate gyrus	4	–41	28	<0.001	3.74
		R precuneus	8	–64	31	0.002	2.94

Results from SPM-99 are listed by clusters and in decreasing order of peak *Z* score value. Cluster size is indicated by the *k* value, which represents the number of significant voxels in the particular cluster. L = left; R = right.

normalization into standard Talairach and Tournoux's space (Talairach and Tournoux, 1988), reapplying the parameters estimated from the normalization of the original PET data using the standard PET template of SPM-99, and to a reslicing of 2 × 2 × 2 mm. The corrected and spatially normalized sets were then smoothed with a 14 mm isotropic Gaussian filter to blur individual variations in gyral anatomy and to increase the signal-to-noise ratio.

Statistical analysis

Principal analyses

The correlations between each memory score on one hand, and GM density and PET data on the other hand were then assessed in four independent analyses (encoding-GM density, retrieval-GM density, encoding-PET and retrieval-PET). Using the 'single-subject: covariates only' routine of SPM-99, with the memory subscore as covariate, correlations were computed across the 21 MCI patients. The 'proportional scaling' routine was applied to the PVE-corrected PET data to control for individual variation in global ^{18}FDG uptake; these normalized and PVE-corrected data will be referred to as 'ncCMRglc' in what follows. For all statistical analyses, only those voxels with values >80% of the mean for the whole brain were selected, and only positive correlations were assessed using a statistical threshold (uncorrected for multiple tests) of $P < 0.005$ for the voxels and of $P < 0.01$ for the clusters, to limit the number of statistical tests and the attending risk of false positives. The use of an uncorrected threshold of P (voxel-level) < 0.005 may not fully protect against results due to chance, but would be more suitable for clinical research with relatively small samples of patients than the more conservative $P < 0.001$. In contrast to activation studies, a more liberal threshold has been used previously with the same correlative approach by our group (Desgranges *et al*., 1998*a*) as well as by other groups (O'Brien *et al*., 1992; Grasby *et al*., 1993). Anatomical localization was according to both the standard template of SPM-99 and Talairach's Atlas, using M. Brett's set of linear transformations (see www.mrc-cbu.cam.ac.uk/Imaging/mnispace.html).

Complementary analyses

To ensure that the correlations were not due either to an age or to a disease severity effect on the variables, we performed the same analyses, but adding age or MMSE score as nuisance variable, so as to control for their potential confounding effects. Moreover, to support the specificity of the observed correlations, we also calculated the correlations with encoding using retrieval performance as nuisance variable, and the correlations with retrieval using encoding performance as nuisance variable.

Since all these correlations were obtained in separate analyses, we used Steiger's test (Steiger, 1980) to assess statistically the differences between these non-independent correlations. This test allows assessment of whether variable A is significantly more strongly correlated with variable B than variable C, taking into account correlation coefficients between both A and B (rAB), and A and C (rAC), as well as the correlation coefficient between B and C (rBC). A t value is calculated from the following equation:

Table 3 *Coefficients of the correlations between test scores and imaging values in the most significant peaks of the principal analyses (A) and of the partial correlations between the same variables adding age, MMSE or the other cognitive test as nuisance variable (B)*

	GM density				ncCMRglc		
	Encoding		Retrieval		Encoding		Retrieval
Regions	R HCP	L HCP	R HCP	L HCP	R HCP	L HCP	PCC
Talairach coordinates (*x*,*y*,*z*)	30,–3,–18	–18,1,–15	34,–26,–7	–26,–14,–14	28,–28,–10	–20,–3,–15	–6,–55,29
A. Principal analyses	0.731	0.592	0.720	0.700	0.630	0.617	0.729
B. Nuisance variable effects							
Age	0.713	0.563	0.748*	0.677	0.637	0.710	0.734
MMSE	0.684	0.632	0.672	0.583	0.607	0.854*	0.732
Test	0.720	0.560	0.721	0.668	0.635	0.613	0.784

Steiger tests (Steiger, 1980) were used to compare the correlation coefficients of the principal analyses with each other as well as each coefficient of the partial correlations with the corresponding correlation coefficient of the principal analyses (i.e. the value at the top of the same column). Significant differences ($P < 0.05$) are indicated by asterisks (note that there is no significant difference between correlation coefficients of the principal analyses). L = left; R = right; PCC = posterior cingulate cortex; HCP = hippocampal area.

$t = (r\mathrm{AB} - \mathrm{rAC})\cdot\sqrt{[(\mathrm{N} - 1)(1 + r\mathrm{BC})/(2((\mathrm{N} - 1)/(\mathrm{N} - 3))\cdot|\mathrm{R}| + ((r\mathrm{AB} + r\mathrm{AC})^2/4)(1 - r\mathrm{BC})^3]}$

with $|\mathrm{R}| = (1 - r\mathrm{AB}^2 - r\mathrm{AC}^2 - r\mathrm{BC}^2) + (2\cdot r\mathrm{AB}\cdot r\mathrm{AC}\cdot r\mathrm{BC})$

This test was used specifically to assess: (i) the asymmetry of the correlations, by comparing each significant correlation in one hemisphere with the equivalent correlation in the opposite hemisphere (obtained at a more liberal threshold if not significant); (ii) the effect of controlling for age, MMSE and encoding or retrieval performances, by comparing the correlations obtained with and without nuisance variable introduction ('nuisance variable effect'); (iii) the differences between MRI and PET correlations, by comparing each significant correlation with GM density, with the correlation with the ncCMRglc values at the same coordinates, and conversely ('imaging modality effect'); and (iv) the differences between encoding versus retrieval correlations, by comparing each significant correlation with one cognitive test with the correlation between the same GM density or ncCMRglc values and the second test ('test effect').

For the sake of completeness, we also compared the memory, MRI and PET profiles of the MCI group with those of partially overlapping samples of healthy controls (see characteristics of each sample in Table 1). Since comparisons of both memory test performances were assessed in separate statistical tests, we also performed an ANOVA (analysis of variance) in order to determine whether any difference between the degree of encoding versus retrieval impairment was statistically significant.

Results

The results of the comparisons between MCI and controls for memory, MRI and PET data will be briefly presented before addressing the correlations, which are the main impetus in this study.

Memory scores in MCI patients

Compared with data from 30 age-matched normal controls (Table 1), performance of the MCI patients was significantly decreased for both the encoding subtest (mean ± SD: 14.8 ± 1.2 and 12.8 ± 1.6, respectively; 13.5% decrease; $P < 0.001$, Student *t* test) and the retrieval subtest (mean ± SD: 7.5 ± 1.5 and 6.3 ± 2.3, respectively; 16% decrease; $P = 0.04$, Student *t* test). The 2 (subject group: MCI, control) × 2 (test: encoding, retrieval) mixed ANOVA with repeated measures showed a significant main effect of the subject group across the tests [$F(1–49) = 17.96$, $P < 0.001$], a significant effect of the test [$F(1–49) = 553.51$, $P < 0.001$], but no significant interaction between test and group [$F(1–49) = 1.98$, $P = 0.17$].

Grey matter loss in MCI patients (for details see Chételat et al., 2002)

The GM data set of the MCI patients was compared with that of 22 healthy controls (see Table 1), using the 'compare-populations: 1 scan/subjects (two-sample *t* tests)' routine of SPM-99. Results obtained using the optimized VBM method of Good *et al*. (2001; data not shown) were very similar to those detailed in another report (Chételat *et al*., 2002), obtained from the same sample, but using the standard VBM method as described in Baron *et al*. (2001*a*). Briefly, the most significant clusters of GM loss in MCI were found in the HCP (including amygdala, anterior hippocampus and Brodmann area 34) bilaterally, extending into the neighbouring temporal neocortex.

Metabolic pattern in MCI patients

The ncCMRglc data set of the MCI patients was compared with that of 13 healthy controls using the 'compare-populations: 1 scan/subjects (analysis of covariance; ANCOVA)'

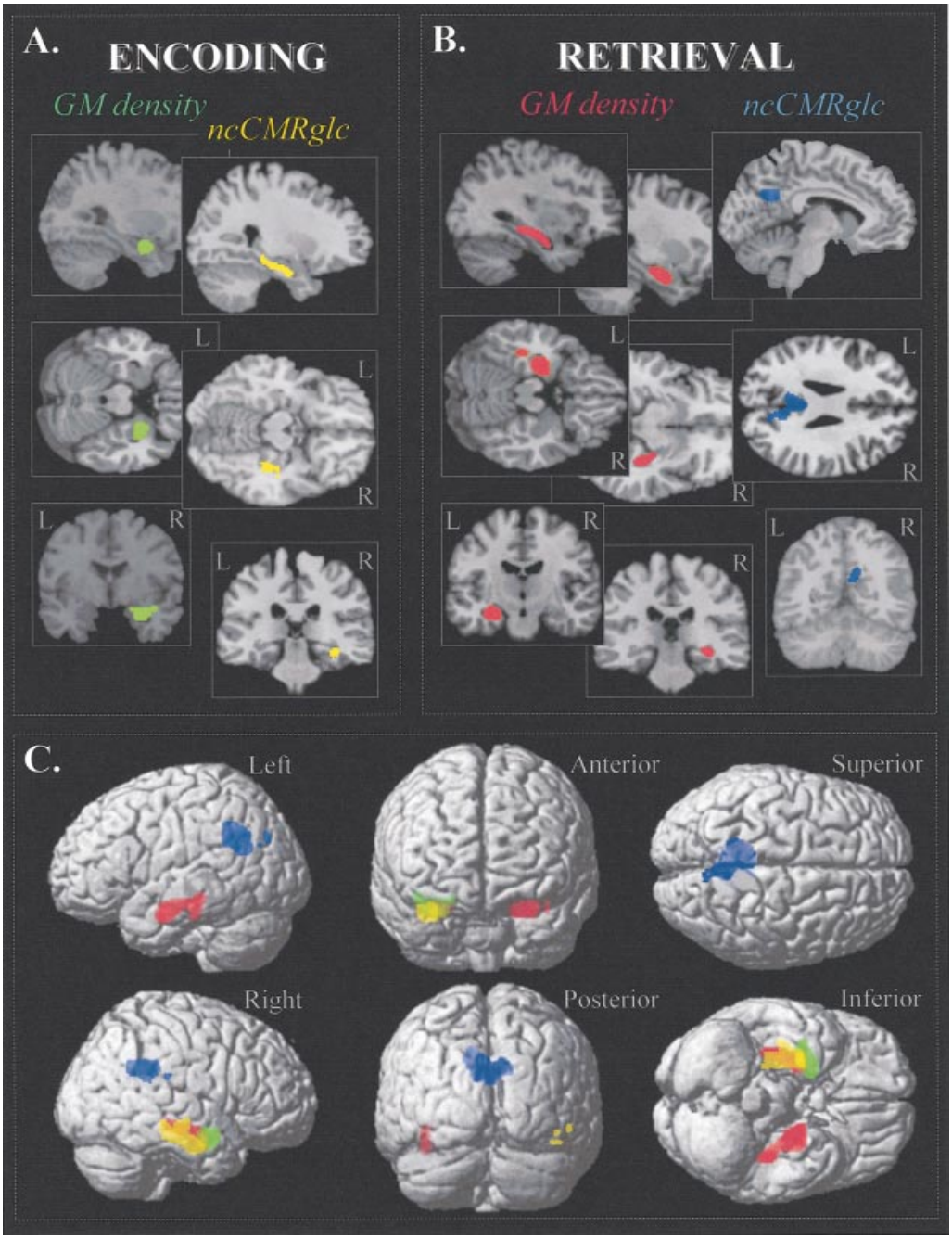

Fig. 1 (**A**) Anatomical localization of the peaks of significant correlations between encoding performance and both GM density and ncCMRglc in the right hippocampal region (in green and yellow, respectively), and (**B**) between retrieval performance and both bilateral hippocampal GM density and posterior cingulate ncCMRglc (in red and blue, respectively), as projected onto sagittal, axial and coronal sections of a normal MRI set spatially normalized into the standard SPM-99 template. (**C**) Three-colour SPM-99 display of surface rendered from six viewpoints showing the superposition of the four significant cognitive correlations mentioned above using SPM-99.

and 'proportional scaling' routines of SPM-99, with age introduced as 'nuisance variable' because of a significant between-group difference (see Table 1). At the uncorrected P (voxel-level) < 0.005 and P (cluster-level) < 0.01 cut-off, the comparison revealed a single peak of hypometabolism in the vicinity of the right precuneus/posterior cingulate cortex [Brodmann areas 7/31; Talairach coordinates: $x = 8$, $y = –55$, $z = 32$; P (uncorrected; cluster-level) < 0.001; Z score = 3.79; cluster size $k = 555$ voxels; P (corrected; cluster-level) = 0.015]. Note that the left (Talairach coordinates: –20,–2,–20) HCP ncCMRglc was also decreased using a more liberal threshold of P (voxel-level, uncorrected) < 0.01

Table 4 *Correlation coefficients between test scores and values of both imaging modalities in each of the most significant peaks of the principal analyses*

	GM density				ncCMRglc		
	Encoding		Retrieval		Encoding		Retrieval
Regions	R HCP	L HCP	R HCP	L HCP	R HCP	L HCP	PCC
Talairach coordinates (*x*,*y*,*z*)	30,–3,–18	–18,1,–15	34,–26,–7	–26,–14,–14	28,–28,–10	–20,–3,–15	–6,–55,29
MRI	0.731	0.592	0.720	0.700	0.537	0.367	0.217*
PET	0.505	0.354	0.365*	0.453	0.630	0.617	0.729

The asterisks indicate significant differences ($P < 0.05$; Steiger test) between the correlation coefficients obtained from GM density versus ncCMRglc values in the same stereotaxic coordinates (i.e. between the two values of the same column). See Table 3 for details and abbreviations.

Table 5 *Correlation coefficients between imaging values in the most significant peaks of the principal analysis, and either encoding or retrieval performances*

	GM density				ncCMRglc		
	Encoding		Retrieval		Encoding		Retrieval
Regions	R HCP	L HCP	R HCP	L HCP	R HCP	L HCP	PCC
Talairach coordinates (*x*,*y*,*z*)	30,–3,–18	–18,1,–15	34,–26,–7	–26,–14,–14	28,–28,–10	–20,–3,–15	–6,–55,29
Encoding	0.731	0.592	0.122*	0.451	0.630	0.617	0.083*
Retrieval	0.565	0.303	0.720	0.700	0.214*	0.117*	0.729

The asterisks indicate significant differences ($P < 0.05$; Steiger test) between the correlation coefficients obtained with one or the other test (i.e. between the two values of the same column). See Table 3 for details and abbreviations.

[cluster-level uncorrected $P = 0.84$; Z score = 2.51; cluster size $k = 3$ voxels; P (corrected; cluster-level) = 1].

Correlations between memory scores and ncCMRglc (principal analyses)

Correlations were assessed with and without the ambidextrous patient. Apart from a slightly lower statistical significance in the latter analysis, identical findings were obtained from these two analyses. Therefore, only results including all the patients ($n = 21$) will be reported in what follows.

The clusters of significant positive correlations with GM density and ncCMRglc for each subtest are listed in Table 2, and their respective correlation coefficients are reported in Table 3A. For the encoding subtest, significant correlations were found with GM density as well as with ncCMRglc in the right HCP, extending into the temporal neocortex (see Fig. 1). For the retrieval subtest, correlations with GM loss involved the bilateral HCP, and that with ncCMRglc concerned the bilateral posterior cingulate cortex, extending into the precuneus and retrosplenial area (without an independent peak, but see Fig. 1).

Comparisons between correlations (complementary analyses)

The results of the Steiger test used to compare the different correlations are reported in Tables 3–5, listing the correlation coefficients of the principal and complementary analyses. These results show, first, a lack of significant difference among the correlations of the principal analyses (Table 3A), including the right and left hemispheric correlation comparisons. Secondly, concerning the effects of the nuisance variables (Table 3B), the encoding right HCP GM density and encoding left HCP ncCMRglc correlations were significantly higher when controlling for age and MMSE, respectively. Thirdly, two significant differences were found when assessing the imagery modality effect, showing that correlations with retrieval were lower with ncCMRglc than with GM density in the right HCP region, and lower with GM density than with ncCMRglc in the posterior cingulate (Table 4). Fourthly, regarding the test effect (Table 5), correlations were significantly lower with encoding than with retrieval for the right HCP GM density and the posterior cingulate ncCMRglc, and lower with retrieval than with encoding for both HCP ncCMRglc.

Discussion

Altogether, our findings reveal both encoding and retrieval deficits in MCI, together with predominant HCP atrophy and posterior cingulate hypometabolism. The encoding impairment correlated with HCP atrophy and metabolism, while retrieval deficits related to both HCP atrophy and posterior cingulate hypometabolism. Before addressing the results of the principal correlation analyses, some methodological

issues regarding the results of the complementary analyses will be first addressed, and the memory, MRI and PET profiles of MCI patients will be briefly discussed.

Methodological issues and complementary analyses

The use of statistical tests comparing the different results obtained from separate analyses reveals the relative degree of these several between-group differences or memory-imaging correlations. The complementary analyses mainly confirmed the apparent general pattern of between-analyses differences. More specifically, they showed the following results:

(i) No significant difference between encoding and retrieval deficits (ANOVA analysis). Regarding the GM density and ncCMRglc profiles, they were reported for information, but our study was not designed to address the relative degree of each impairment. Indeed, since the GM density and ncCMRglc comparisons used different samples of controls, with age being added as nuisance variable in the latter, but not in the former analyses, we were unable to perform an ANOVA in order to seek statistical advice on the relative degree of GM density and ncCMRglc decreases. For this reason, the apparent discordance between these cerebral profiles of alteration may only reflect a difference in the variances, and not necessarily in the magnitude, of the effects, and is therefore discussed with caution in what follows.

(ii) An absence of significant difference among the principal analysis correlations (Table 3A), including no right–left difference. Therefore, the hemispheric lateralization of the HCP correlations with retrieval capacity is only apparent and will not be discussed in what follows.

(iii) A dissociation between atrophy versus hypometabolism correlation with memory performances (Table 4), with significant differences in the correlations between retrieval performances and GM density versus ncCMRglc in both the right HCP and the posterior cingulate area.

(iv) A dissociation between encoding versus retrieval correlations with ncCMRglc, with significant differences for the HCP (right and left) and the posterior cingulate area (Table 5), suggesting the specific implication of these structures in either encoding or retrieval, respectively. This regional specificity is supported further by the addition of the second test as nuisance variable, showing a similar degree of correlation. Since it is statistically supported only in selected voxels of most significant correlations, this dissociation should be replicated so as to be accepted as proven. Concerning GM density, the structural correlates for encoding and retrieval deficits were mainly similar, both implicating the HCP. However, in the right HCP peak of correlation between GM density and retrieval, the correlation with encoding was significantly lower, suggesting that the specific location of these correlations differed. More specifically, it involves only the most anterior part of the HCP (amygdala and hippocampal head) for encoding, while it is spatially more extended for retrieval. This result will be commented upon below in the section on encoding correlations.

Finally, relying on correlations between cognitive performances and imaging for identifying cognitively dissociated brain regions has some limitations. Correlation analyses are based on the variance in the measured variables. Thus, despite the use of statistical support to reinforce the specificity of the correlations, potential differences in the variability of the memory scores or the neuroimaging values may have affected our results. Moreover, one can also argue that the correlations observed do not reflect specific relationships between variables, but instead were induced by a similar effect of another parameter, such as ageing or disease severity, on these variables. To assess the effect of such potential confounds, we separately added age and MMSE score as nuisance variable. The results showed no significant negative effect of the nuisance variables on the correlations, arguing in favour of specific relationships (Table 3B).

Memory impairment profile in MCI patients

The present study shows that the episodic memory impairment of our MCI sample involved encoding and retrieval deficits of similar severity. These findings contrast with those of Wang and Zhou (2002) reporting more severe encoding than retrieval deficits. This discrepancy might be related to the fact that MCI patients had significant deficits in orientation, praxis and language besides memory in this latter study, thus not strictly corresponding to the amnestic MCI *per se* as in our study. Moreover, differences in the tasks used to assess retrieval (i.e. a recognition task, instead of a free recall task in our study), as well as in the materials used for memory evaluation (pictures instead of words) may also have given rise to differences in the findings. Our results suggesting that encoding and retrieval are both decreased in patients with amnestic MCI are similar to findings in Alzheimer's disease, which is characterized by concomitant encoding and retrieval deficits as compared with controls, with, however, a predominance of the former.

GM loss pattern in MCI patients

The pattern of GM atrophy as reflected using VBM revealed the HCP and temporal neocortex as the most significantly altered structures in our MCI sample. This finding is highly consistent with previous MRI studies on MCI showing significant HCP atrophy using the regions-of-interest method (Convit *et al*., 1997; Jack *et al*., 2000; De Santi *et al*., 2001; for a review see Chételat and Baron, 2003). Our results also agree with the well-established early neuropathological alteration of medial temporal structures, already present in normal ageing, and even more conspicuous in MCI (Braak and Braak, 1996; Delacourte *et al*., 1999), spreading toward the temporal

neocortical areas, in most subjects with isolated memory impairment (for further discussion see Chételat *et al*., 2002).

ncCMRglc pattern in MCI patients

Only the right precuneus/posterior cingulate area was significantly hypometabolic in our sample of MCI patients. Significant metabolic reduction was also found in the same area in patients at a pre-dementia stage of Alzheimer's disease (Minoshima *et al*., 1997), and similar results were reported in two SPECT (single photon emission computed tomography) studies (Johnson *et al*., 1998; Kogure *et al*., 2000), as well as in non-demented subjects at risk of developing Alzheimer's disease, such as ApoE4 carriers (Reiman *et al*., 1996; Small *et al*., 2000), and asymptomatic subjects carrying the presenilin-1 mutation (Johnson *et al*., 2000). As previously proposed (Minoshima *et al*., 1997), the discrepancy between the neuropathological alteration of this region, which appears somewhat delayed in the evolution of Alzheimer's disease (Delacourte *et al*., 1999), and its early metabolic reduction, argues toward synaptic dysfunction over and above neuronal lesions in the posterior cingulate gyrus. In a preliminary study of the voxel-based comparison of structural and functional imaging data in patients with Alzheimer's disease, we reported that posterior cingulate cortex ncCMRglc reduction was significantly more pronounced than GM density change in this area (Baron *et al*., 2001*b*). Using voxel-based analyses of MRI and SPECT data, Matsuda *et al*. (2002) also reported a discordance between morphological and functional changes. These authors concluded that functional changes may be caused partly by remote effects from the morphologically altered areas with decreased connectivity, and partly by a compensatory response by neuronal plasticity. As the posterior cingulate area is highly interconnected with the HCP structures, its functional impairment could be due, at least in part, to a remote effect from damage within the HCP, where Alzheimer's disease pathology occurs initially (Meguro *et al*., 1999). We failed to evidence statistically significant HCP ncCMRglc reduction in our study using our selected threshold. Very discrepant findings have been reported using functional imaging with regard to HCP alterations in MCI and Alzheimer's disease, and this apparent discrepancy between predominant HCP structural damage and questionable or delayed neocortical functional alteration remains to be elucidated (Matsuda, 2001). Several hypotheses have been proposed, including a methodological bias (see for example Convit *et al*., 1997; Ishii *et al*., 1998; De Santi *et al*., 2001). More precisely, the sampling of the whole HCP region, without distinguishing its several parts, may have contributed to negative findings in previous studies using the regions-of-interest approach, and the spatial resolution degradation due to both normalization and smoothing may explain negative findings in studies using SPM such as ours.

Memory correlations with GM density and ncCMRglc

Overall, our results firstly highlight a dissociation between atrophy versus hypometabolism impact on retrieval performances. Thus, significant correlations with retrieval performance concerned posterior cingulate metabolism, but not GM density, and HCP GM density, but not metabolism (see also Fig. 1). This dissociation, formally confirmed by the complementary statistical analyses (see above), suggests distinct interpretation for structural versus functional correlations. PET measurements of ncCMRglc reflect local baseline integrated synaptic activity and therefore both neuronal lesions and synaptic dysfunction, while VBM only assesses structural changes. Cognitive performances probably depend on how the underlying structures function, as better reflected by metabolism, whereas correlations with atrophy may reveal a more indirect relationship reflecting atrophy-induced functional disruption in the area subtending the task. More specifically, in our study, the GM density correlations point to structures whose atrophy induces a remote functional perturbation itself involved in the memory impairment, revealed by the correlations with ncCMRglc.

Secondly, our results reveal a dissociation between encoding and retrieval correlations with ncCMRglc, involving the HCP in the former and the posterior cingulate in the latter analyses, again formally confirmed by the complementary analyses (see above). Encoding and retrieval deficits therefore appear to be subtended by functional alteration in distinct areas, successively addressed in the following paragraphs.

Performance in the encoding subtest correlated with right HCP atrophy and hypometabolism. The role of the HCP in memory is clearly established from a convergent broad and multidisciplinary literature (Milner, 1972; Squire and Zola-Morgan, 1991), and correlations between episodic memory deficits and HCP metabolism have been reported previously in Alzheimer's disease (see Introduction). Moreover, the preferential implication of the HCP in the encoding process is consistent with activation studies on normal subjects showing that medial temporal activation is more frequent with encoding than with retrieval (Tulving and Markowitsch, 1997; Desgranges *et al*., 1998*b*; Cabeza and Nyberg, 2000), as well as with one previous activation study in MCI also reporting HCP dysfunction in an encoding task (Small *et al*., 1999). Similarly, functional MRI studies have reported decreased activation in the HCP during episodic memory encoding tasks in Alzheimer's disease (Rombouts *et al*., 2000; Kato *et al*., 2001; Sperling *et al*., 2003). The present findings suggest that metabolic integrity of the HCP may be crucial for the encoding of information in MCI, whereas retrieval difficulty would not be directly subtended by HCP dysfunction. Concerning the functional specialization of the HCP according to its antero-posterior axis, and although our study was not specifically designed to assess this issue, we generally found a preferential implication of the anterior part

of the HCP in correlations with memory scores (see Fig. 1), consistent with several volumetric MRI studies showing the specific implication of the hippocampal head, but not of its posterior part, in verbal episodic memory (O'Driscoll *et al*., 2001; Hackert *et al*., 2002). More specifically, the HCP correlation with encoding specifically concerned its anterior part in the present study (complementary analyses, see above). This finding fits well with one previous functional MRI report in young subjects suggesting the crucial role of the hippocampal head in novelty encoding (Strange *et al*., 1999), as well as with the HIPER (hippocampal Encoding/Retrieval) model (Lepage *et al*., 1998).

Concerning the retrieval subtest, performance correlated with both HCP atrophy and posterior cingulate metabolism. Previous reports highlight the role of limbic areas in memory deficits in Alzheimer's disease (Desgranges *et al*., 1998*a*; for a review see Deweer *et al*., 2001), suggesting that the underlying pathological processes in MCI may be similar to that involved in Alzheimer's disease. The involvement of the posterior cingulate region in memory has been clearly established by studies in amnesia (Valenstein *et al*., 1987; Aupée *et al*., 2001). Furthermore, our finding of a specific implication of this area in the retrieval subtest impairment fits well with previous activation studies on normal subjects documenting its role in memory retrieval (Mottaghy *et al*., 1999; Bernard *et al*., 2001; for a review see Cabeza and Nyberg, 2000). With respect to the remote effect hypothesis (see above), our findings further suggest a mechanism whereby retrieval impairment in MCI is subtended by posterior cingulate functional disruption as a result of decreased connectivity with the atrophied HCP. This interpretation is reinforced by a recent study assessing, with SPM, the correlation between GM density values in the voxels of greatest hippocampal atrophy (obtained when comparing Alzheimer's disease patients with controls using VBM), and cerebral blood flow SPECT measurement obtained during a verbal memory task (Garrido *et al*., 2002). These authors showed significant correlations between hippocampal atrophy and functional activity reduction, notably in the posterior cingulate area.

Conclusion

The present findings reveal, for the first time in the same study and by means of objective and comprehensive methodology, both the structural and metabolic substrates of episodic memory deficits in MCI. First, our findings disclose a dissociation between metabolic and structural correlates, suggesting distinct interpretations. Secondly, they highlight partly distinct neural substrates for encoding and retrieval deficits. On the one hand, decreased encoding performances appear to depend on structural and functional disruption of the HCP, i.e. the earliest site of neuropathological changes in Alzheimer's disease. On the other hand, retrieval deficits appear related to HCP atrophy and posterior cingulate dysfunction, the latter being the only significantly hypometabolic area in our MCI sample. Thus, the early structural alteration of the hippocampal region may induce, via decreased connectivity, the observed posterior cingulate functional disruption, leading to retrieval impairment. More generally, the neural basis of memory impairment in MCI, involving the limbic structures as revealed by this investigation, is reminiscent of that previously shown in Alzheimer's disease, further reinforcing the idea that amnestic MCI is the main forerunner of Alzheimer's disease.

Acknowledgements

We wish to thank Ms F. Mézenge, Ms M. H. Noël, Ms M. C. Onfroy, Mr G. Perchey, Mr D. Luet, Mr O. Tirel, Ms R. M. Marié, Ms A. Blondel, Ms C. Giry, Mr A. Traifi-Delarue and Mrs F. Leblond for their help in this study, and the anonymous referees for their constructive comments. This work was supported by INSERM U.320, Ministère de la Santé (PHRC, Principal Investigator: J.-C.B.), Ministère de l'éducation nationale, and the Fondation France-Alzheimer.

References

Almkvist O, Basun H, Backman L, Herlitz A, Lannfelt L, Small B, et al. Mild cognitive impairment—an early stage of Alzheimer's disease? J Neural Transm Suppl 1998; 54: 21–9.

Ashburner J, Friston KJ. Multimodal image coregistration and partitioning—a unified framework. Neuroimage 1997; 6: 209–17.

Ashburner J, Friston KJ. Voxel-based morphometry: the methods. Neuroimage 2000; 11: 805–21.

Ashburner J, Friston KJ. Why voxel-based morphometry should be used. Neuroimage 2001; 14: 1238–43.

Aupée AM, Desgranges B, Eustache F, Lalevée C, de la Sayette V, Viader F, et al. Voxel-based mapping of brain hypometabolism in permanent amnesia with PET. Neuroimage 2001; 13: 1164–73.

Baron JC, Chételat G, Desgranges B, Perchey G, Landeau B, de la Sayette V, et al. In vivo mapping of gray matter loss with voxel-based morphometry in mild Alzheimer's disease. Neuroimage 2001a; 14: 298–309.

Baron JC, Chételat G, Perchey G, Poline JB, Landeau B, Desgranges B, et al. Does resting glucose hypometabolism exceed gray matter atrophy in early Alzheimer's disease (AD)? A voxel-based comparison of structural and functional imaging data. Neuroimage 2001b; 13: S771.

Bernard F, Desgranges B, Platel H, Baron JC, Eustache F. Contributions of frontal and medial temporal regions to verbal episodic memory: a PET study. Neuroreport 2001; 12: 1737–41.

Braak H, Braak E. Evolution of the neuropathology of Alzheimer's disease. Acta Neurol Scand Suppl 1996; 165: 3–12.

Cabeza R, Nyberg L. Imaging cognition II: an empirical review of 275 PET and fMRI studies. J Cogn Neurosci 2000; 12: 1–47.

Carlesimo GA, Mauri M, Graceffa AM, Fadda L, Loasses A, Lorusso S, et al. Memory performances in young, elderly, and very old healthy individuals versus patients with Alzheimer's disease:

evidence for discontinuity between normal and pathological aging. J Clin Exp Neuropsychol 1998; 20: 14–29.

Chételat G, Baron JC. Early diagnosis of Alzheimer's disease: contribution of structural neuroimaging. [Review]. Neuroimage 2003; 18: 525–41.

Chételat G, Desgranges B, de la Sayette V, Viader F, Eustache F, Baron JC. Mapping gray matter loss with voxel-based morphometry in mild cognitive impairment. Neuroreport 2002; 13: 1939–43.

Content A, Mousty P, Radeau M. Brulex: une base de données lexicales informatisée pour le français écrit et parlé. Ann Psychol 1990; 90: 551–66.

Convit A, De Leon MJ, Tarshish C, De Santi S, Tsui W, Rusinek H, et al. Specific hippocampal volume reductions in individuals at risk for Alzheimer's disease. Neurobiol Aging 1997; 18: 131–8.

Delacourte A, David JP, Sergeant N, Buée L, Wattez A, Vermersch P, et al. The biochemical pathway of neurofibrillary degeneration in aging and Alzheimer's disease. Neurology 1999; 52: 1158–65.

Deloche G, Hannequin D. Test de dénomination orale d'images DO80. Paris: éd. Française; 1997.

De Santi S, De Leon MJ, Rusinek H, Convit A, Tarshish CY, Roche A, et al. Hippocampal formation glucose metabolism and volume losses in MCI and AD. Neurobiol Aging 2001; 22: 529–39.

De Santi S, de Leon MJ, Rusinek H, Golomb J, Convit A, Tarshish C, et al. Selective medial temporal lobe pathology in cases at risk for Alzheimer's disease: diagnostic role of positron emission tomography. In: Iqbal K, Mortimer JA, Winblad B, Wisniewski HM, editors. Research advances in Alzheimer's disease and related disorders. Chichester (UK): John Wiley; 1995. p. 173–80.

Desgranges B, Baron JC, de la Sayette V, Petit-Taboué MC, Benali K, Landeau B, et al. The neural substrates of memory systems impairment in Alzheimer's disease. A PET study of resting brain glucose utilization. Brain 1998a; 121: 611–31.

Desgranges B, Baron JC, Eustache F. The functional neuroanatomy of episodic memory: the role of the frontal lobes, the hippocampal formation, and other areas. Neuroimage 1998b; 8: 198–213.

Desgranges B, Baron JC, Lalevée C, Giffard B, Viader F, de la Sayette V, et al. The neural substrates of episodic memory impairment in Alzheimer's disease as revealed by 18FDG-PET: relationship to degree of deterioration. Brain 2002; 125: 1116–24.

Deweer B, Pillon B, Pochon JB, Dubois B. Is the HM story only a 'remote memory'? Some facts about hippocampus and memory in humans. Behav Brain Res 2001; 127: 209–24.

Eustache F, Rioux P, Desgranges B, Marchal G, Petit-Taboué MC, Dary M, et al. Healthy aging, memory subsystems and regional cerebral oxygen consumption. Neuropsychologia 1995; 33: 867–87.

Eustache F, Desgranges B, Lalevée C. Clinical evaluation of memory. [French]. Rev Neurol (Paris) 1998; 154 Suppl 2: S18–32.

Eustache F, Desgranges B, Giffard B, de la Sayette V, Baron JC. Entorhinal cortex disruption causes memory deficit in early Alzheimer's disease as shown by PET. Neuroreport 2001; 12: 683–5.

Folstein MF, Folstein SE, McHugh PR. 'Mini-mental state'. A practical method for grading the cognitive state of patients for the clinician. J Psychiatr Res 1975; 12: 189–98.

Gabrieli JE, Brewer JB, Desmond JE, Glover GH. Separate neural bases of two fundamental memory processes in the human medial temporal lobe. Science 1997; 276: 264–6.

Garrido GE, Furuie SS, Buchpiguel CA, Bottino CM, Almeida OP, Cid CG, et al. Relation between medial temporal atrophy and functional brain activity during memory processing in Alzheimer's disease: a combined MRI and SPECT study. J Neurol Neurosurg Psychiatry 2002; 73: 508–16.

Golden CJ. The stroop color and word test: a manual for clinical and experimental uses. Chicago: Stoelting; 1978.

Good CD, Johnsrude IS, Ashburner J, Henson RN, Friston KJ, Frackowiak RS. A voxel-based morphometric study of ageing in 465 normal adult human brains. Neuroimage 2001; 14: 21–36.

Grasby PM, Frith CD, Friston KJ, Bench C, Frackowiak RS, Dolan RJ. Functional mapping of brain areas implicated in auditory–verbal memory function. Brain 1993; 116: 1–20.

Grober E, Buschke H. Genuine memory deficits in dementia. Dev Neuropsychol 1987; 3: 13–36.

Hackert VH, den Heijer T, Oudkerk M, Koudstaal PJ, Hofman A, Breteler MM. Hippocampal head size associated with verbal memory performance in nondemented elderly. Neuroimage 2002; 17: 1365–72.

Ishii K, Sasaki M, Yamaji S, Sakamoto S, Kitagaki H, Mori E. Relatively preserved hippocampal glucose metabolism in mild Alzheimer's disease. Dement Geriatr Cogn Disord 1998; 9: 317–22.

Jack CR, Petersen RC, Xu Y, O'Brien PC, Smith GE, Ivnik RJ, et al. Rates of hippocampal atrophy correlate with change in clinical status in aging and AD. Neurology 2000; 55: 484–9.

Johnson KA, Jones K, Holman BL, Becker JA, Spiers PA, Satlin A, et al. Preclinical prediction of Alzheimer's disease using SPECT. Neurology 1998; 50: 1563–71.

Johnson SC, Saykin AJ, Baxter LC, Flashman LA, Santulli RB, McAllister TW, et al. The relationship between fMRI activation and cerebral atrophy: comparison of normal aging and Alzheimer disease. Neuroimage 2000; 11: 179–87.

Kato T, Knopman D, Liu H. Dissociation of regional activation in mild AD during visual encoding: a functional MRI study. Neurology 2001; 57: 812–6.

Kogure D, Matsuda H, Ohnishi T, Asada T, Uno M, Kunihiro T, et al. Longitudinal evaluation of early Alzheimer's disease using brain perfusion SPECT. J Nucl Med 2000; 41: 1155–62.

Langley LK, Madden DJ. Functional neuroimaging of memory: implications for cognitive aging. Microsc Res Tech 2000; 51: 75–84.

Lepage M, Habib R, Tulving E. Hippocampal PET activations of memory encoding and retrieval: the HIPER model. Hippocampus 1998; 8: 313–22.

Loeb C, Gandolfo C. Diagnostic evaluation of degenerative and vascular dementia. Stroke 1983; 14: 399–401.

Matsuda H. Cerebral blood flow and metabolic abnormalities in Alzheimer's disease. Ann Nucl Med 2001; 15: 85–92.

Matsuda H, Kitayama N, Ohnishi T, Asada T, Nakano S, Sakamoto S, et al. Longitudinal evaluation of both morphologic and functional changes in the same individuals with Alzheimer's disease. J Nucl Med 2002; 43: 304–11.

McKhann G, Drachman D, Folstein M, Katzman R, Price D, Stadlan EM. Clinical diagnosis of Alzheimer's disease: report of the NINCDS-ADRDA Work Group under the auspices of Department of Health and Human Services Task Force on Alzheimer's Disease. Neurology 1984; 34: 939–44.

Meguro K, Blaizot X, Kondoh Y, Le Mestric C, Baron JC, Chavoix C. Neocortical and hippocampal glucose hypometabolism following neurotoxic lesions of the entorhinal and perirhinal cortices in the non-human primate as shown by PET. Implications for Alzheimer's disease. Brain 1999; 122: 1519–31.

Milner B. Disorders of learning and memory after temporal lobe lesions in man. Clin Neurosurg 1972; 19: 421–46.

Minoshima S, Giordani B, Berent S, Frey KA, Foster NL, Kuhl DE. Metabolic reduction in the posterior cingulate cortex in very early Alzheimer's disease. Ann Neurol 1997; 42: 85–94.

Mottaghy FM, Shah NJ, Krause BJ, Schmidt D, Halsband U, Jancke L, et al. Neuronal correlates of encoding and retrieval in episodic memory during a paired-word association learning task: a functional magnetic resonance imaging study. Exp Brain Res 1999; 128: 332–42.

Müller-Gartner HW, Links JM, Prince JL, Bryan RN, McVeigh E, Leal JP, et al. Measurement of radiotracer concentration in brain gray matter using positron emission tomography: MRI-based correction for partial volume effects. J Cereb Blood Flow Metab 1992; 12: 571–83.

O'Brien JT, Eagger S, Syed GM, Sahakian BJ, Levy R. A study of regional cerebral blood flow and cognitive performance in Alzheimer's disease. J Neurol Neurosurg Psychiatry 1992; 55: 1182–7.

O'Driscoll GA, Florencio PS, Gagnon D, Wolff AV, Benkelfat C, Mikula L, et al. Amygdala–hippocampal volume and verbal memory in first-degree relatives of schizophrenic patients. Psychiatry Res 2001; 107: 75–85.

Oldfield RC. The assessment and analysis of handedness: the Edinburgh inventory. Neuropsychologia 1971; 9: 97–113.

Perani D, Bressi S, Cappa SF, Vallar G, Alberoni M, Grassi F, et al. Evidence of multiple memory systems in the human brain. A ^{18}FDG PET metabolic study. Brain 1993; 116: 903–19.

Petersen RC, Jack CR Jr, Xu YC, Waring SC, O'Brien PC, Smith GE, et al. Memory and MRI-based hippocampal volumes in aging and AD. Neurology 2000; 54: 581–7.

Petersen RC, Doody R, Kurz A, Mohs RC, Morris JC, Rabins PV, et al. Current concepts in mild cognitive impairment. Arch Neurol 2001; 58: 1985–92.

Raz N, Gunning-Dixon FM, Head D, Dupuis JH, Acker JD. Neuroanatomical correlates of cognitive aging: evidence from structural magnetic resonance imaging. Neuropsychology 1998; 12: 95–114.

Reiman EM, Caselli RJ, Yun LS, Chen K, Bandy D, Minoshima S, et al. Preclinical evidence of Alzheimer's disease in persons homozygous for the epsilon 4 allele for apolipoprotein E. N Engl J Med 1996; 334: 752–8.

Rey A. Test de copie d'une figure complexe de A. Rey. Paris: éd. Française; 1959.

Rombouts SA, Barkhof F, Veltman DJ, Machielsen WC, Witter MP, Bierlaagh MA, et al. Functional MR imaging in Alzheimer's disease during memory encoding. AJNR Am J Neuroradiol 2000; 21: 1869–75.

Small SA, Perera GM, DeLaPaz R, Mayeux R, Stern Y. Differential regional dysfunction of the hippocampal formation among elderly with memory decline and Alzheimer's disease. Ann Neurol 1999; 45: 466–72.

Small GW, Ercoli LM, Silverman DH, Huang SC, Komo S, Bookheimer SY, et al. Cerebral metabolic and cognitive decline in persons at genetic risk for Alzheimer's disease. Proc Natl Acad Sci USA 2000; 97: 6037–42.

Sperling RA, Bates JF, Chua EF, Cocchiarella AJ, Rentz DM, Rosen BR, et al. fMRI studies of associative encoding in young and elderly controls and mild Alzheimer's disease. J Neurol Neurosurg Psychiatry 2003; 74: 44–50.

Squire LR, Zola-Morgan S. The medial temporal lobe memory system. Science 1991; 253: 1380–6.

Steiger JH. Tests for comparing elements of a correlation matrix. Psychol Bull 1980; 2: 245–51.

Strange BA, Fletcher PC, Henson RN, Friston KJ, Dolan RJ. Segregating the functions of human hippocampus. Proc Natl Acad Sci USA 1999; 96: 4034–9.

Talairach J, Tournoux P. Co-planar stereotaxic atlas of the human brain. 3-dimensional proportional system: an approach to cerebral imaging. Stuttgart: Thieme; 1988.

Tulving E, Markowitsch HJ. Memory beyond the hippocampus. Curr Opin Neurobiol 1997; 7: 209–16.

Valenstein E, Bowers D, Verfaellie M, Heilman KM, Day A, Watson RT. Retrosplenial amnesia. Brain 1987; 110: 1631–46.

Wang QS, Zhou JN. Retrieval and encoding of episodic memory in normal aging and patients with mild cognitive impairment. Brain Res 2002; 924: 113–5.

Wright IC, Ellison ZR, Sharma T, Friston KJ, Murray RM, McGuire PK. Mapping of grey matter changes in schizophrenia. Schizophr Res 1999; 35: 1–14.

Received August 5, 2002. Revised February 13, 2003.
Second revision April 9, 2003. Accepted April 11, 2003